Articles

Contribution from the Department of Chemistry,
Washington State University, Pullman, Washington 99164

Electronic Structure of *trans*-$[Cr(ox)_2(py)_2]^-$ by the Xα-Scattered Wave Method

WILLIAM D. WHEELER and RONALD D. POSHUSTA*

Received November 7, 1984

The electronic structure of *trans*-$[Cr(ox)_2(py)_2]^-$ (ox = oxalate, py = pyridine) as calculated by the spin-polarized SCF-Xα-SW method is reported. The ground state of the ion is found to be $^4B_{1g}$ for the assumed D_{2h} equilibrium geometry. The calculated electronic absorption spectrum associated with metal d-d and pyridine $\pi-\pi^*$ transitions is in good agreement with experiment. The calculated energies of the ligand to metal charge-transfer transitions, however, are grossly underestimated. This is not uncommon in Xα-SW calculations and is a result of the metal d orbitals having an energy which is too low compared to that of other orbitals. The ^{53}Cr hyperfine coupling constant is calculated to be 16.0×10^{-4} cm^{-1}, which is a value that is typical for Cr(III) complexes and is probably within a few percent of the correct value. The computed proton (deuteron) NMR shift for the proton that is on the 2(6)-position of the pyridyl ring is in quantitative agreement with experiment, but the shifts computed for the 3(5)- and 4-positions bear little resemblance to experiment. This may be due to excessive mixing of the Cr $3d_{z^2}$ orbital (which is formally unoccupied) into the wave function, which is also a result of the depressed energies of the metal d orbitals and the symmetry of the complex. The calculated molecular **g** tensor agrees with experimental values obtained for a large number of closely related complexes.

Introduction

Although Cr(III) complexes have been studied for many years, it has only recently been possible to structurally characterize them by nuclear magnetic resonance techniques.[1] The dramatic reduction in line width associated with the smaller magnetic moment of the deuteron[2] has made it possible to characterize a variety of Cr(III) compounds by ^2H NMR spectroscopy when ^2H is substituted for ^1H on the coordinating ligand.

In Table I, the deuteron chemical shifts of several deuterated Cr(III)-pyridine complexes in solution are shown.[3] For comparison the chemical shifts of two other metal-pyridine complexes, one containing Ni(II) and the other Mo(III), have also been included in Table I. The similarity in the pattern of shifts of the Cr(III) complexes to that of the Mo(III) complex ($3d^3$ and $4d^3$ electronic configurations, respectively) and the very different pattern of shifts shown by the Ni(II) complex ($3d^8$) suggests a common mechanism for the Cr(III) and Mo(III) complexes that is dependent on the electronic structure.

Previous investigations have suggested that reliable electronic structures and magnetic hyperfine parameters can be obtained by the SCF-Xα-SW method. Weber et al.[4] have calculated the $^{59}Co(II)$ hyperfine tensor of $Co(cp)_2$[8] and found it to agree with experiment to within 10%. They observed, however, that the Fermi contact term is sensitive to both the metal to cp ring distance and to the sphere radii of the atoms. Daul and Weber[5] have calculated the complete **g** and **A** tensors of axially perturbed square-planar complexes of Co(II) by using wave functions and parameters derived from Xα-SW calculations of Co(acacen) have found nearly quantitative agreement with experiment. Sontum and Case[6] have calculated magnetic resonance parameters for the metal, nitrogen, and pyrrole hydrogen atoms of Cu(II) and Ag(II) porphines. Although the spin densities at the metal and pyrrole hydrogen nuclei were found to be underestimated by about 30%, their calculations were able to reproduce trends that are observed experimentally for these compounds. They found that the Ag porphine showed smaller metal hyperfine coupling and larger proton and nitrogen hyperfine couplings as compared to those of the Cu porphine, because of the increased covalency of the bonds between the Ag ion to the porphine ligand. More recently, Sontum et al.[7] have found that the correct ordering of the contact shifts is predicted for both the pyrrole and meso protons of Fe(II) porphine. Although their results were not quantitatively correct, they are certainly very encouraging in the sense that the Xα-SW method provides a useful theoretical model for the study of the optical and magnetic properties of transition-metal complexes.

We report calculations on *trans*-$[Cr(ox)_2(py)_2]^-$ by the Xα-SW method. This molecule is one of several Cr(III)-pyridine complexes for which experimental data are readily available. Our results provide an initial theoretical foundation for structural and magnetic properties of these Cr(III) complexes and for future structural studies of more complicated systems. Our calculated NMR parameters, however, disagree with experiment; we analyze

Table I. Deuteron NMR Spectra of Some Cr(III)-Pyridine-d_5 Complexes in Solution

complex[b]	chem shift (rel integration)[a]		
	2(6)[c]	3(5)	4
trans-$[Cr(ox)_2(py)_2]^-$	-63	10	-22
cis-$[Cr(ox)_2(py)_2]^-$	-65	14	-27
trans-$[Cr(mal)_2(py)_2]^-$[1]	-71	11	-24
mer-$[Cr(NCS)_3(py)_3]$	-68 (3)	11 (2), 9 (1)	-27 (3)
trans-$[Cr(NCS)_4(py)_2]^-$	-67	10	-24
trans-$[CrF_2(py)_4]^+$	-78	13	-32
mer-$[CrF_3(py)_3]$	-68 (3)	16 (1), 14 (2)	-23 (2), -26 (1)
mer-$[CrCl_3(py)_3]$	-72	9	-26
mer-$[MoCl_3(py)_3]$	-84 (2), -86 (1)	36 (2), 37 (1)	-68 (2), -73 (1)
trans-$[Ni(acac)_2(py)_2]$[2]	39	17	10

[a] In ppm vs. Me_4Si. An external standard of C^2HCl_3 was assigned a chemical shift of 7.24 ppm. Positive shifts are to high frequency. [b] Unless otherwise noted, all spectra are from this laboratory.[3] [c] Position on the pyridine ring.

(1) Wheeler, W. D.; Kaizaki, S.; Legg, J. I. *Inorg. Chem.* **1982**, *21*, 3248. Green, C. A.; Bianchini, R. J.; Legg, J. I. *Inorg. Chem.* **1984**, *23*, 2713. Wheeler, W. D.; Legg, J. I. *Inorg. Chem.* **1984**, *23*, 3798. Wheeler, W. D.; Legg, J. I. *Inorg. Chem.* **1985**, *24*, 1292.
(2) Johnson, A.; Everett, G. W., Jr. *J. Am. Chem. Soc.* **1972**, *94*, 1419. Everett, G. W.; Johnson, A. *J. Am. Chem. Soc.* **1972**, *94*, 6397.
(3) Kaizaki, S.; Legg, J. I., unpublished data.
(4) Weber, J.; Goursot, A.; Penigault, E.; Ammeter, J. H.; Bachmann, J. *J. Am. Chem. Soc.* **1982**, *104*, 1491.
(5) Daul, C.; Weber, J. *Helv. Chim. Acta* **1982**, *65*, 2486.
(6) Sontum, S. F.; Case, D. A. *J. Phys. Chem.* **19828** *86*, 1596. See also: Case, D. A.; Karplus, M. *J. Am. Chem. Soc.* **1977**, *99*, 6182.
(7) Sontum, S. F.; Case, D. A.; Karplus, M. *J. Chem. Phys.* **1983**, *79*, 2881.
(8) Abbreviations: py = pyridine; cp = cyclopentadienyl; mal = malonate; ox = oxalate; acac = acetylacetonate; en = ethylenediamine; acacen = *N,N'*-ethylenebis(acetylacetone iminato).

0020-1669/85/1324-3100$01.50/0

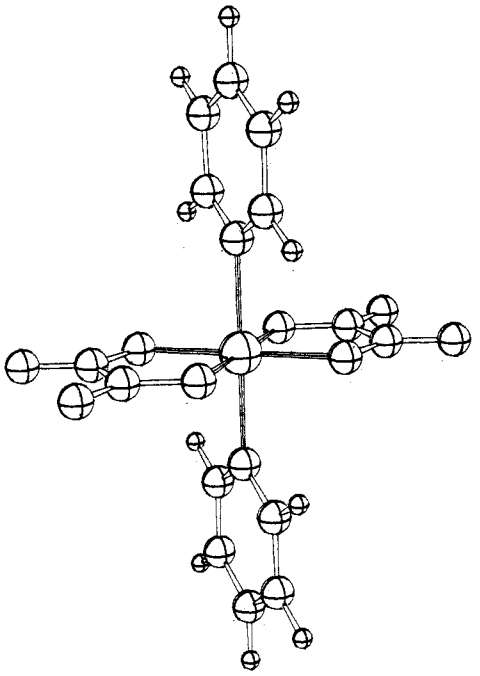

Figure 1. Coordination geometry of *trans*-$[Cr(ox)_2(py)_2]^-$. Coordinate axes and atomic positions are given in Table II.

Table II. Coordinates, Radii, and α Parameters[a] of the Unique Atoms

atom	x	y	z	radius	α
III[b]	0.0	0.0	0.0	12.5350	0.753 44
Cr	0.0	0.0	0.0	2.2396	0.713 52
O_1	2.4168	2.7316	0.0	1.6975	0.744 47
C	1.3315	4.9566	0.0	1.5458	0.759 28
O_2	2.4315	7.0256	0.0	1.6971	
N	0.0	0.0	3.9646	1.6453	0.751 97
C_1	2.2017	0.0	5.2383	1.6668	
C_2	2.2741	0.0	7.9113	1.6999	
C_3	0.0	0.0	9.2321	1.6914	
H_1 (2(6))[c]	3.9898	0.0	4.2390	1.2725	0.777 25
H_2 (3(5))	4.0306	0.0	8.9543	1.2715	
H_3 (4)	0.0	0.0	11.2673	1.2677	

[a] Values in au. [b] Outer sphere. [c] Positions on the pyridine ring.

the reasons for this disagreement.

Experimental Section

trans-$K[Cr(ox)_2(py)_2]\cdot 2H_2O$ was prepared from *trans*-$K[Cr(ox)_2(OH_2)]\cdot 3H_2O$[9] by a previously reported method.[10] Anal. Calcd for $KCrC_{14}H_{14}N_2O_{10}$: C, 36.44; H, 3.06; N, 6.07; Cr, 11.27. Found: C, 36.32; H, 3.05; N, 6.01; Cr, 11.43.

The room-temperature absorption spectrum of the compound dissolved in water was recorded on a Varian/Cary 219 spectrophotometer. The wavelength maxima (in nm) and molar absorptivities for the complex are 521 (32.3), 376 (30.7), and 259 (7060). These are in close agreement with a previously reported spectrum.[11]

Method of Calculation

The SCF–Xα–SW method will not be described here, as many excellent discussions have already appeared in the literature.[12,13] The calculations were performed with the general release VAX-IBM version 1 of the XASW package, written by D. A. Case and M. Cook and obtained from M. Cook. One hundred iterations were required to reach convergence (a relative change in the potential of 10^{-4}) for the spin-unrestricted ground-state calculation. A typical iteration required about 350 CPU seconds on an Amdahl 470/V8.

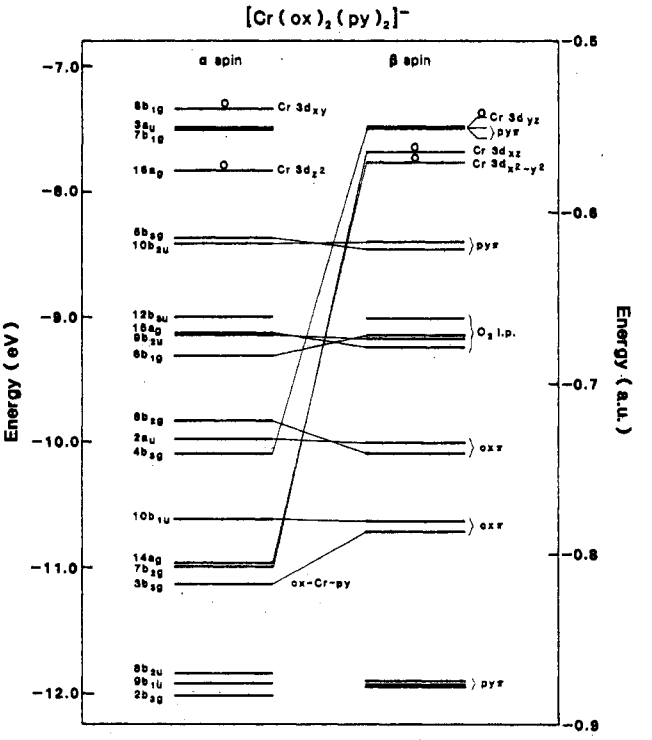

Figure 2. Molecular orbital diagram for *trans*-$[Cr(ox)_2(py)_2]^-$. The MOs have been separated into two manifolds with the α spin orbitals on the left side of the diagram and the β spin on the right. The symmetries and *sequence numbers* of the α spin orbitals are indicated on the left-hand side of the diagram while the *shapes* of the orbitals are indicated to the right. The lines connecting the α and β spin MOs are drawn from an α spin MO to a β spin MO with the corresponding symmetry and *shape*. Open circles indicate unoccupied orbitals. Abbreviation: l.p., lone pair.

The symmetry of the title compound was assumed to be D_{2h} and is shown in Figure 1. The atomic coordinates and parameter values used in the calculation are summarized in Table II. The coordinates of the pyridine C and N atoms and the Cr–N distance were set to an average of the bond lengths and angles of the two pyridines that are trans to each other in crystalline *mer*-$Cr(Cl)_3(py)_3$.[14] The C–H bond lengths were taken from the microwave structure of free pyridine.[15] The geometry of the pyridine fragment is very similar to that used in a previous Xα–SW calculation on free pyridine.[16] The coordinates of the oxalate C and O atoms and the Cr–O distance were derived by averaging the bond lengths and angles reported for the crystal structure of *trans*-$K[Cr(ox)_2(PH_2)_2]\cdot 3H_2O$.[17]

The α parameters in the atomic regions are those of Schwarz and Slater,[18] with the intersphere and outer-sphere values chosen as the average of the atomic values weighted by the number of valence electrons. The sphere radii were determined by the nonempirical method of Norman[19] from neutral-atom charge densities and scaled by a factor of 0.88. The outer sphere was chosen to be tangent to the sphere of the hydrogen on the 4-position of pyridine (H_3). A "Watson" sphere with a radius equal to the outer sphere and a charge of +1 was used to approximate the effects of any surrounding counterions or solvent.[20]

Calculations were carried out with use of partial waves up through $l = 4$ for the outer sphere, $l = 3$ on Cr, $l = 2$ on C, N, and O, and through $l = 1$ on H. The number of partial waves used in this calculation is quite large compared to that of other calculations, which generally use only enough partial waves to correspond to a minimal angular basis in LCAO theory.[4-7]

(9) Kauffman, G. B.; Faoro, D. *Inorg. Synth.* **1977**, *17*, 147.
(10) Meisenheimer, J. *Justus Liebigs Ann. Chem.* **1924**, *438*, 217.
(11) Casula, M.; Illuminati, G.; Ortaggi, G. *Inorg. Chem.* **1972**, *11*, 1062.
(12) Slater, J. C. "The Calculation of Molecular Orbitals"; Wiley: New York, 1979. Slater, J. C. "Quantum Theory of Molecules and Solids"; McGraw-Hill: New York, 1974; Vol. IV.
(13) Connolly, J. W. D. *Mod. Theor. Chem.* **1977**, *7*, 105. Johnson, K. H. *Adv. Quantum Chem.* **1973**, *7*, 143. Johnson, K. H. *Annu. Rev. Phys. Chem.* **1975**, *26*, 29. Case, D. A. *Annu. Rev. Phys. Chem.* **1982**, *33*, 151.
(14) Pennington, W. T.; Cordes, A. W., personal communication.
(15) Bak, B.; Hansen-Nygaard, L.; Rastrup-Anderson, J. *J. Mol. Spectrosc.* **1958**, *2*, 361.
(16) Case, D. A.; Cook, M.; Karplus, M. *J. Chem. Phys.* **1980**, *73*, 3294.
(17) Van Niekerk, J. N.; Schoening, F. R. L. *Acta Crystallogr.* **1951**, *4*, 35.
(18) Schwarz, K. *Phys. Rev. B: Solid State* **1972**, *5*, 2466. Schwarz, K. *Theor. Chim. Acta* **1974**, *34*, 225. Slater, J. C. *Int. J. Quantum Chem. Symp.* **1973**, *7*, 533.
(19) Norman, J. G., Jr. *Mol. Phys.* **1976**, *31*, 1191.
(20) Watson, R. E. *Phys. Rev.* **1958**, *14*, 1108.

Results and Discussion

Description of the Electronic Structure. The *trans*-$[Cr(ox)_2(py)_2]^-$ ion is a 197-electron system which formally consists of a Cr(III) ion (21e) bound to two oxalate dianions (2 C, 4 O; 46e) and two pyridine molecules (1 N, 5 C, 5 H; 42e). The complete electronic configuration consists of 28 atomic core and 69 molecular orbitals (MOs), which are "doubly occupied" (see below), and three singly occupied MOs. The latter orbitals are predominantly Cr 3d in character. The valence orbital energies and atomic contributions to the total charge are shown in Table III. The latter property corresponds to the shape of spatial distribution of the orbital. Figure 2 shows the valence molecular orbital diagram for energies between −12 and −7 eV. The ground configuration is found to be $|14a_g,7b_{2g},4b_{3g}|$, which corresponds to a $^4B_{1g}$ state under D_{2h} symmetry. The spin-polarized (UHF) procedure used in this calculation generates a wave function that is not rigorously an eigenfunction of the S^2 operator. The single determinant, however, is irreducible under D_{2h} symmetry, corresponding to the B_{1g} irreducible representation. We believe that the wave function does approximate a quartet since the only strongly polarized orbitals are those that are predominantly metal 3d in character and all of the other orbitals are approximately doubly occupied.

Pairs of occupied spin-up (α) orbitals and corresponding occupied spin-down (β) orbitals of the same symmetry and sequence number and with approximately the same energy and spatial distribution are referred to as being doubly occupied. Most orbitals are doubly occupied, but some, with significant Cr 3d character, show a spin polarization of the α and β MOs by as much as 3.5 eV (namely the following orbitals: $14a_g\alpha$, $15a_g\beta$; $8b_{1g}\alpha$, $8b_{1g}\beta$; $7b_{2g}\alpha$, $8b_{2g}\beta$; $3,4b_{3g}\alpha$, $3,5b_{3g}\beta$). Similar spin polarizations were found for both the triplet and quintet states of Fe(II) porphine.[7]

There are two doubly occupied pyridine π orbitals ($3a_u$, $7b_{1g}$) that lie $\simeq$0.35 eV above unoccupied Cr $3d_{z^2}$, $3d_{xz}$, $3d_{x^2-y^2}$ orbitals ($16a_g\alpha$, $15a_g\beta$, $8b_{2g}\beta$). The orbitals within a given irreducible representation are filled in order of increasing, energy but the HOMOs of some representations lie above the LUMOs of others. Coulomb and exchange interactions keep the orbitals from filling in order of absolute energy in much the same way that high-spin configurations in metal complexes are stabilized when pairing energies are larger than $10Dq$. Localizing the charge onto the Cr ion in the $16a_g$ MO (56% Cr 3d) raises its energy above that of the delocalized $3a_u$. A transition-state calculation connecting the $3a_u\alpha$ MO to the lower lying $16a_g\alpha$ MO supports this conclusion.[21]

The singly occupied spin-up Cr 3d orbitals lie $\simeq$3.5 eV below the doubly occupied HOMO. Cu(II) and Fe(II) porphines also show this type of behavior, where the occupied spin-up metal d orbitals lie about 1 eV below the HOMO. Aizman and Case have shown by atomic calculations on first-row metals that the Xα exchange correlation potential favors configurations with more d electrons over those with less.[22] The indication was that the metal d-orbital energies are too low by as much as 2.2 eV for Cr^+ (the net charge on Cr in the present calculation is +0.9, Table III), and they concluded that this should carry over into molecular calculations. This effect, the depressed energies of the metal d orbital in Xα calculations, plays an important role in computing ligand to metal (and metal to ligand) charge-transfer energies[22] and may also be important in determining the distribution of spin in *trans*-$[Cr(ox)_2(py)_2]^-$, as will be discussed below.

Most of the molecular orbitals can be seen to be approximately localized on fragments such as oxalate, pyridine, or metal orbitals. Exceptions to this are the $3b_{3g}$ and $4b_{3g}$ MOs, which are delocalized over most of the molecule. Chemically interesting orbitals are those arising from the π orbitals of pyridine (which have b_{1g}, b_{3g}, a_u, and b_{2u} symmetry), π orbitals of oxalate (which have b_{2g}, b_{3g}, a_u, and b_{1u} symmetry), and the orbitals with predominantly Cr 3d character (a_g, b_{1g}, b_{2g}, and b_{3g} symmetry). The Cr $3d_{yz}$ (b_{3g}) orbital, which has the proper symmetry to π bond with both pyridine and oxalate, mixes so strongly with both the pyridine π and oxalate π orbitals that it is impossible to distinguish which of the $3b_{3g}$ or $4b_{3g}$ MOs belongs to the $t_{2g}(O_h)$[23] manifold (Table III). In an investigation of the spectra of $[Cr(py)_4XY]$ compounds, Glerup et al.,[24] using the angular-overlap model, found a metal–pyridine π-bonding interaction for Ni(II) and Cr(III). They interpreted this interaction as a π back-bonding of metal orbitals with the pyridine π^* orbitals. Careful examination of the results presented in Table 103,[25] however, reveals that the Cr(III) ion interacts with the π *bonding* orbitals of pyridine and *not* the antibonding orbitals which lie above −7 eV. This would still be true even if the energies of the Cr 3d orbitals were not anomalously low since the spin polarization of 3.5 eV would more than offset the 2.2-eV increase in orbital energy.

Electronic Absorption Spectrum. Table IV summarizes the calculated electronic transitions of *trans*-$[Cr(ox)_2(py)_2]^-$ in the ultraviolet and visible regions of the spectrum. Transition energies have been computed by taking differences in orbital energies (Koopmans' theorem), E_K, and where indicated, by taking Slater's transition-state method, E_{TS},[12] and the relaxation energy, E_R ($E_{TS} - E_K$), is estimated. The transitions in Table IV are arranged into three categories. The first category includes the oxalate and pyridine π–π^* transitions, which are allowed and are observed as intense bands in the UV. In the second category are the metal d–d or ligand field transitions. These are formally forbidden by symmetry but gain intensity through vibronic interactions. They are observed experimentally as broad weak bands in the visible and near-UV portion of the spectrum. Finally, the ligand to metal charge-transfer transitions are listed. Although these transitions are allowed, they are not usually observed for Cr(III) complexes since they apparently lie at energies above the UV region of the spectrum. The experimental spectrum along with the calculated ligand field and pyridine π–π^* transitions are shown in Figure 3.

In addition to information shown in Figure 3, there is a band with very high intensity ($\epsilon > 100000$) at 201 nm that is not shown. This agrees well with the lowest energy oxalate π–π^* transition, which is computed to be at 191 nm (Table IV), although this transition could also be due to or include ligand to metal charge transfer.

The eight peaks clustered between 220 and 290 nm are associated with the pyridine π–π^* transitions. The calculated and experimental spectra are in good agreement for this set of transitions also. It appears that the small change in the charge distribution associated with the pyridine π–π^* transitions results in small relaxation energies, Table 104.[25]

If we turn to the ligand field bands, it is readily apparent from the calculated spectrum (Figure 3) that both the $^4A_{2g} \rightarrow {}^4T_{2g}$ and the $^4A_{2g} \rightarrow {}^4T_{1g}$ transitions (O_h) undergo large splittings[3] due to the lowering of symmetry from octahedral. The transition from the $^4A_{2g}$ state to the $^4B_{2g}$ component (D_{4h}) of the $^4T_{2g}$ state is observed experimentally at 521 nm with the transition to the ^4E_g component shifted to higher energy at 377 nm. The transition from the $^4A_{2g}$ state to the $^4A_{2g}$ component of the $^4T_{1g}$ state is experimentally observed at about 405 nm with the transition to the ^4E_g component shifted to about 340 nm. It is tempting to make comparisons to ligand field theory and suggest that the pyridine is a weaker ligand than the oxalate in the ligand field sense since the $E_g(D_{4h})$ components are at higher energies than the A_{2g} and B_{2g}. The $16a_g$ MO, which is predominantly the Cr $3d_{z^2}$ orbital, lies below the $8b_{1g}$ MO, which is largely the Cr $3d_{xy}$ orbital. This also indicates that oxalate is a stronger ligand than pyridine. In light of the strong interactions of the metal ion with both pyridine and oxalate, comparisons to ligand field theory may be unwar-

(21) This calculation was only converged far enough to determine that the transition energy was positive.
(22) Aizman, A.; Case, D. A. *Inorg. Chem.* **1981**, *20*, 528.
(23) The environment of the chromium ion is approximately octahedral, O_h, for which the basis orbitals of the Cr are irreducible. Thus, in some cases the MOs can be identified with their octahedral counterparts.
(24) Glerup, J.; Monsted, O.; Schaffer, C. E. *Inorg. Chem.* **19768**, *15*, 1399; **1980**, *19*, 2855.
(25) See for instance: Jorgensen, W. L.; Salem, L. In "The Organic Chemists Book of Orbitals"; Academic Press: New York, 1973; p 263.

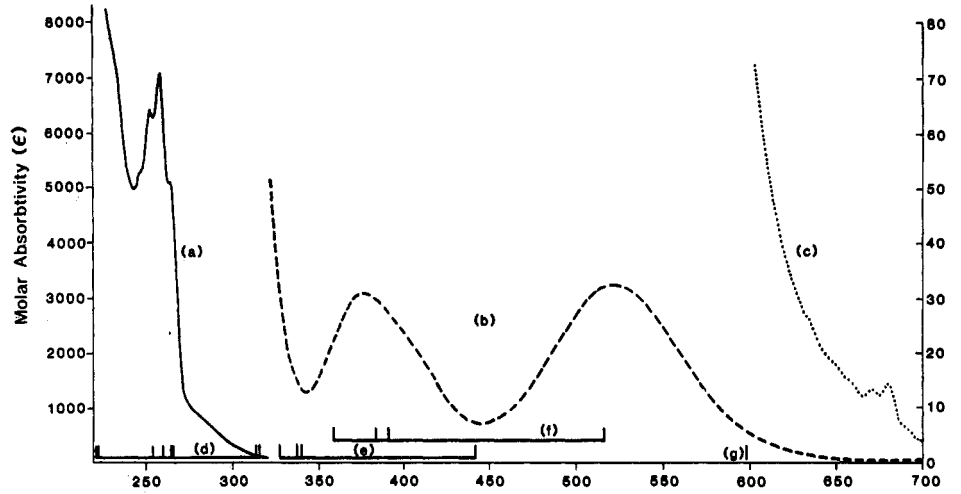

Figure 3. Experimental electronic absorption spectrum of *trans*-$[Cr(ox)_2(py)_2]^-$: (a) portion of the spectrum associated with the pyridine $\pi-\pi^*$ transitions (refer to the scale on the left-hand side of the figure); (b) portion of the spectrum associated with the metal d–d transitions (refer to the scale on the right-hand side of the figure); (c) spectrum in (b) magnified 15 times. Calculated absorption spectrum: (d) pyridine $\pi-\pi^*$ transitions; (e) $^4A_{2g} \rightarrow {}^4T_{1g}$ (O_h) d–d transitions; (f) $^4A_{2g} \rightarrow {}^4T_{2g}$ d–d transitions; (g) $^4A_{2g} \rightarrow {}^2E_g$ d–d transition.

ranted since it presumes the interactions of the metal with the ligands to be small.

Table IV shows that the relaxation energies range from −9300 to +1200 cm^{-1} within the Cr d–d transitions. The reduced symmetry of the complex splits the single $^4A_{2g} \rightarrow {}^4T_{2g}$ transition under O_h symmetry into three whose relaxation energies range from 200 to 1200 cm^{-1}. Thus, relaxation energies can vary considerably within a given manifold of transitions as well as within a given category. This is significant because some workers assume that the relaxation energy is constant within a category and apply the relaxation energy found for one transition to all of the transitions in that class.[7,22]

The calculated ligand to metal charge-transfer energies are shown in the last part of Table IV. It can be seen that these transitions are not well described either by orbital energy differences or by transition-state calculations. This behavior is not entirely unexpected since it is known that the Xα local density function tends to place metal d orbitals about 2.2 eV too low in energy, as previously reported.[22] Correcting for these low orbital energies by adding 2.2 eV (18 000 cm^{-1}) to the orbital energy differences of the charge-transfer transitions moves them from the IR and visible region of the spectrum to the visible and UV region. Adding in the increased relaxation energy associated with these "new" higher energy orbitals could well put them out in the vacuum UV, in better agreement with experiment.

Molecular g Tensor. The molecular **g** tensor is computed by following the method outlined by Norman et al.[26] The general expression for g_{zz} given through second order in perturbation theory is[27]

$$g_{zz} = 2 + \frac{1}{S}\sum_{n\neq p}\sum_{k}\frac{\langle\Phi_p|l_k^z|\Phi_n\rangle\langle\Phi_n|\xi_k(r)l_k^z|\Phi_p\rangle}{\epsilon_p - \epsilon_n} \qquad (1)$$

The sum over k includes all atoms with spin–orbit constants $\xi_k(r)$ and the summations over n and p in general include both occupied and virtual molecular orbitals. Eacn MO is a linear combination of "atomiclike" orbitals, Φ_i, and is written as $|\Phi_p\rangle = |a_g\rangle = \beta|z^2\rangle + \gamma|x^2 - y^2\rangle$ + ligand contributions, $|b_{1g}\rangle = \alpha|xy\rangle$ + ligand contributions, $|b_{2g}\rangle = \alpha|xz\rangle$ + ligand contributions, and $|b_{3g}\rangle = \alpha|yz\rangle$ + ligand contributions. Symmetry considerations limit the number of matrix elements that need to be included. Under D_{2h} symmetry the angular momentum operators l^x, l^y, and l^z transform as b_{3g}, b_{2g}, and b_{1g}, respectively. Thus to compute the zz component of the **g** tensor, the only nonvanishing matrix elements are $\langle a_b|l^z|b_{1g}\rangle$ and $\langle b_{2g}|l^z|b_{3g}\rangle$ (the u,u terms are ignored because none involve Cr 3d orbitals). Since the Cr(III) ion is the only atom/ion with an appreciable free ion spin–orbit coupling constant λ (taken to be 230 cm^{-1}),[28,29] our discussion will consider the Cr(III) ion only. Considering that $\xi(r)$ falls off approximately as $1/r^3$, terms containing $|\xi_k(r)l_k^z|\Phi_j\rangle$ $(k \neq j)$ are small and will also be neglected. The remaining contributions are from "atomic-like" orbitals which have p, d, or f character on the Cr atom. The contributions from p and f orbitals will be small since the Cr 3p orbitals lie at −54 eV and the Cr 4f orbitals are expected to be near the continuum. The final expression for g_{zz} is

$$g_{zz} = 2 + \tfrac{2}{3}\lambda\sum_p \alpha_p^2 f_p(\Gamma,\Gamma')\sum_n \beta_n^2/(\epsilon_p - \epsilon_n) \qquad (2)$$

where f_p is a number (between 0.27 and 4) that depends on the symmetries Γ and Γ' of the orbital pair chosen[30] and $\epsilon_p - \epsilon_n$ is the orbital energy difference.[31] The parameters α_p^2 and β_n^2 are the squares of the MO coefficients on the Cr ion and are obtained from the MS–Xα charge distribution of the orbitals in question. The only orbitals considered here contain >10% of the charge on the Cr(III) ion. The α's in this discussion are the coefficients on the Cr(III) ion in the MO which contains an unpaired electron while the β's are the coefficients from doubly occupied and virtual MOs. The terms in the summation enter the resulting expression with + and − signs due to the energy denominator, in agreement with the general rule that terms between singly occupied and virtual orbitals will have negative contributions to the **g** tensor while terms between singly and doubly occupied orbitals provide positive contributions. The g_{xx}, g_{yy}, and g_{zz} components of the **g** tensor is then essentially isotropic. The magnetic properties of several related Cr(III)–pyridine complexes have been measured, and all show **g** tensors that are almost isotropic with g values between 1.97 and 1.99.[32] These data strongly suggest that the **g** tensor calculated here will be found to be in good agreement with experiment.

Hyperfine Structure. In the analysis of the hyperfine structure only the Fermi contact contributions are considered. This is justified for Cr(III) complexes as follows. The ground state for Cr(III) complexes under octahedral symmetry is $^4A_2$. Since there is no splitting of the ground state via spin–orbit coupling (to first order), the zero-field splittings of Cr(III) complexes are small

(26) Norman, J. G.; Renzoni, G. E.; Case, D. A. *J. Am. Chem. Soc.* **1979**, *101*, 5256.
(27) Stone, A. J. *Proc. R. Soc. London, Ser. A* **1963**, *271*, 424.
(28) Carrington, A.; McLachlan, A. D. In "Introduction to Magnetic Resonance"; Chapman and Hall: London, 1980; p 146.
(29) McGarvey, B. R. *Transition Met. Chem. (N.Y.)* **1966**, *3*, 138, 146.
(30) Wheeler, W. D. Ph.D. Dissertation.
(31) Strictly speaking, it is not correct to use orbital energy differences and these should be replaced by energies derived from transition-state calculations. The effect of this on the **g** tensor is small since the relaxation energy is small compared to the transition energy.
(32) Pedersen, E.; Toftlund, H. *Inorg. Chem.* **1974**, *13*, 1602.

Table III. Atomic Contributions to the Total Charge in the Valence MOs of *trans*-$[Cr(ox)_2(py)_2]^-$

MO[d]	energy[b]	charge distribn, %[a]											
		Cr	O_1	C	O_2	N	C_1	C_2	C_3	H_1	H_2	H_3	II[c]
						Total							
		23.1	7.9	5.4	7.9	6.9	5.6	5.7	5.7	1.0	1.0	1.0	8.9
						Spin-Up (α) Orbitals							
$12b_{2u}°$	−2.785	0	0	0	0	1	1	0	1	0	0	0	82
$12b_{1u}°$	−2.806	0	0	0	0	0	0	0	0	0	0	0	88
$4a_u°$	−2.810	0	0	0	0	1	7	9	1	0	0	0	31
$9b_{1g}°$	−2.823	0	0	0	0	1	7	9	1	0	0	0	34
$13b_{3u}°$	−3.319	0	0	0	0	0	0	0	0	0	0	0	91
$17a_g°$	−3.417	0	0	0	0	0	0	0	0	0	0	0	91
$7b_{3g}°$	−3.536	1	0	0	0	8	6	1	9	0	0	0	33
$11b_{2u}°$	−3.603	0	0	0	0	7	6	1	9	0	0	0	37
$6b_{3g}°$	−4.129	0	2	10	6	0	0	0	0	0	0	0	26
$11b_{1u}°$	−4.184	0	2	10	6	0	0	0	0	0	0	0	26
$8b_{1g}°$	−7.342	52	8	0	3	0	0	0	0	0	0	0	4
$3a_u$	−7.485	0	0	0	0	0	10	7	0	0	0	0	31
$7b_{1g}$	−7.495	0	0	0	0	1	10	7	0	0	0	0	31
$16a_g°$	−7.824	56	3	0	0	12	1	0	0	0	0	0	3
$5b_{3g}$	−8.369	1	0	0	0	5	0	8	13	0	0	0	30
$10b_{2u}$	−8.410	0	0	0	0	5	0	8	13	0	0	0	31
$12b_{3u}$	−8.990	0	1	1	20	0	0	0	0	0	0	0	14
$15a_g$	−9.133	2	2	3	16	0	0	0	0	0	0	0	17
$9b_{2u}$	−9.148	0	1	3	17	0	0	0	0	0	0	0	17
$6b_{1g}$	−9.303	10	1	1	17	0	0	0	0	0	0	0	13
$8b_{2g}$	−9.822	11	4	1	14	0	0	0	0	0	0	0	14
$2a_u$	−9.981	0	3	2	16	0	0	0	0	0	0	0	16
$4b_{3g}$	−10.11	35	6	1	6	0	0	0	0	0	0	0	11
$10b_{1u}$	−10.61	0	6	2	12	1	0	0	0	0	0	0	18
$14a_g$	−10.98	81	2	0	1	1	0	0	0	0	0	0	5
$7b_{2g}$	−11.00	67	1	1	3	0	0	0	0	0	0	0	8
$3b_{3g}$	−11.13	34	1	2	5	6	2	1	0	0	0	0	16
$8b_{2u}$	−11.84	0	1	0	0	22	5	1	0	0	0	0	24
$9b_{1u}$	−11.92	4	0	0	1	27	4	3	1	1	1	1	5
$2b_{3g}$	−12.01	13	1	2	2	17	3	1	0	0	0	0	21
$7b_{2u}$	−12.39	5	15	3	2	2	0	0	0	0	0	0	11
$11b_{3u}$	−12.71	4	20	1	1	0	0	0	0	0	0	0	11
$1a_u$	−12.98	0	17	2	1	0	0	0	0	0	0	0	16
$13a_g$	−13.15	16	5	2	1	9	3	3	2	1	1	2	3
						Spin-Down (β) Orbitals							
$12b_{2u}°$	−2.761	0	0	0	0	0	1	0	0	0	0	0	82
$12b_{1u}°$	−2.780	0	0	0	0	0	0	0	0	0	0	0	88
$4a_u°$	−2.798	0	0	0	0	1	7	9	1	0	0	0	31
$9b_{1g}°$	−2.810	0	0	0	0	1	7	9	1	0	0	0	33
$13b_{3u}°$	−3.292	0	0	0	0	0	0	0	0	0	0	0	91
$17a_g°$	−3.389	0	0	0	0	0	0	0	0	0	0	0	90
$7b_{3g}°$	−3.506	1	0	0	0	8	6	1	9	0	0	0	33
$11b_{2u}°$	−3.599	0	0	0	0	7	6	1	9	0	0	0	37
$6b_{3g}°$	−4.119	0	2	10	6	0	0	0	0	0	0	0	26
$11b_{1u}°$	−4.177	0	2	10	6	0	0	0	0	0	0	0	26
$8b_{1g}°$	−4.924	73	5	0	1	0	0	0	0	0	0	0	3
$16a_g°$	−5.384	74	2	0	0	7	0	0	0	0	0	0	3
$5b_{3g}°$	−7.467	78	1	0	0	1	0	1	2	0	0	0	8
$3a_u$	−7.474	0	0	0	0	1	10	7	0	0	0	0	31
$7b_{1g}$	−7.484	0	0	0	0	1	10	7	0	0	0	0	31
$8b_{2g}°$	−7.679	86	1	0	0	0	0	0	0	0	0	0	6
$15a_g°$	−7.753	86	1	0	1	0	0	0	0	0	0	0	6
$10b_{2u}$	−8.392	0	0	0	0	5	0	8	13	0	0	0	31
$4b_{3g}$	−8.460	6	0	0	0	4	1	7	11	0	0	0	29
$12b_{3u}$	−9.010	0	1	1	19	0	0	0	0	0	0	0	14
$6b_{1g}$	−9.140	3	0	1	19	0	0	0	0	0	0	0	14
$9b_{2u}$	−9.171	0	1	3	17	0	0	0	0	0	0	0	17
$14a_g$	−9.241	3	1	3	16	0	0	0	0	0	0	0	17
$2a_u$	−10.01	0	3	2	16	0	0	0	0	0	0	0	16
$7b_{2g}$	−10.09	3	2	2	16	0	0	0	0	0	0	0	16
$10b_{1u}$	−10.63	0	6	2	12	1	0	0	0	0	0	0	18
$3b_{3g}$	−10.72	3	5	3	12	1	0	0	0	0	0	0	19
$8b_{2u}$	−11.90	1	2	0	0	22	5	1	0	0	0	0	23
$9b_{1u}$	−11.92	3	0	0	1	27	4	3	1	1	1	1	5
$2b_{3g}$	−11.94	1	0	1	1	23	5	1	0	0	0	0	24
$7b_{2u}$	−12.32	4	14	3	2	3	1	0	0	0	0	0	11
$11b_{3u}$	−12.66	4	20	1	1	0	0	0	0	0	0	0	11
$13a_g$	−12.82	13	0	0	0	19	5	4	2	1	1	2	0

[a] Percentage of the total occupation within the region indicated. The charge in the outer-sphere region is zero except for the orbitals with a population in the intersphere region of greater than 40%. [b] Energies in electronvolts. [c] The intersphere region. [d] The ° sign indicates that this is a virtual orbital.

Table IV. Calculated Electronic Absorption Spectrum of *trans*-$[Cr(ox)_2(py)_2]^-$

transition	E_K, nm[a]	E_{TS}, nm[b]	E_R, cm^{-1} [c]
Ligand Field Transitions (Forbidden)			
	$^4A_{2g} \rightarrow {}^4T_{2g}$ (O_h)		
$14a_g \rightarrow 16a_g$	394	391	200
$7b_{2g} \rightarrow 16a_g$	391	384	470
$4b_{3g} \rightarrow 16a_g$	546	516	1100
$3b_{3g} \rightarrow 16a_g$	375	359	1200
	$^4A_{2g} \rightarrow {}^4T_{1g}$ (O_h)		
$14a_g \rightarrow 8b_{1g}$	341	340	90
$7b_{2g} \rightarrow 8b_{1g}$	339	337	180
$4b_{3g} \rightarrow 8b_{1g}$	448	442	300
$3b_{3g} \rightarrow 8b_{1g}$	327		
	$^4A_{2g} \rightarrow {}^2E_g$ (O_h)		
$14a_g\alpha \rightarrow 15a_g\beta$	384	598	−9300
$7b_{2g} \rightarrow 8b_{2g}\beta$	373		
$4b_{3g}\alpha \rightarrow 5b_{3g}\beta$	469		
$3b_{3g}\alpha \rightarrow 5b_{3g}\beta$	339		
Pyridine $\pi \rightarrow \pi^*$ Transitions (Allowed)			
$7b_{1g} \rightarrow 4a_u$	265 (265)[d]	265	0
$7b_{1g} \rightarrow 11b_{2u}$	319 (319)	316	300
$5b_{3g} \rightarrow 4a_u$	223 (219)		
$5b_{3g} \rightarrow 11b_{2u}$	260 (255)		
$3a_u \rightarrow 7b_{3g}$	314 (313)		
$3a_u \rightarrow 9b_{1g}$	266 (266)		
$10b_{2u} \rightarrow 7b_{1g}$	254 (254)		
$10b_{2u} \rightarrow 9b_{1g}$	222 (222)		
Oxalate $\pi \rightarrow \pi^*$ Transitions (Allowed)			
$10b_{1u} \rightarrow 6b_{3g}$	191 (190)		
Ligand to Metal Charge-Transfer Transitions (Allowed)			
$10b_{1u} \rightarrow 16a_g$	445		
$9b_{2u} \rightarrow 16a_g$	937		
$12b_{3u} \rightarrow 16a_g$	1060		
$10b_{2u} \rightarrow 16a_g$	2120	911	6260
$2a_u \rightarrow 8b_{1g}$	470		
$9b_{2u} \rightarrow 8b_{1g}$	687		
$12b_{3u} \rightarrow 8b_{1g}$	752	526	5710
$10b_{2u} \rightarrow 8b_{1g}$	1160	609	7800
$3a_u \rightarrow 8b_{1g}$	8670		

[a] The wavelength of the transition as computed from the ground-state orbital energy difference (e.g. Koopmans' theorem). [b] As computed from a transition-state calculation. [c] $(1/E_{TS} = 1/E_K) \times 10^7$. [d] Numbers in parentheses are the wavelengths of the transitions as computed from the energy difference of spin-down orbitals.

(typically less than 1 cm^{-1}). Small zero-field splittings lead to metal contributions to the pseudocontact shift that are negligible (for a $S = {}^3/_2$ system with $r = 5$ Å and $T = 15$ °C, a zero-field splitting of 5.7 cm^{-1} gives a pseudocontact shift of 1 ppm).[33] Ligand contributions to the pseudocontact shift are also zero for the same reason. Second-order effects can couple the ground state to excited states with orbital angular momentum, but these are usually small since the lowest excited states are typically 15 000 cm^{-1} above the ground state.

The hyperfine coupling constants are calculated via the Bloembergen–McConnell equation:[34]

$$\frac{\Delta H}{H} = -\frac{2\pi g\beta S(S+1)}{3h\gamma_n kT} A_n \qquad (3)$$

In this equation A_n is the hyperfine coupling constant, S is the total spin on the ion, g is the free-electron g factor, β is the Bohr magneton, h is Planck's constant, γ_n is the magnetic moment of the nucleus n, k is Boltzmann's constant, and T is the absolute temperature. For $T = 300$ K and $S = {}^3/_2$, the contact shift (in ppm) is $\Delta H/H = (-1.96 \times 10^5)s_n(0)$, where $s_n(0)$ is the spin density at nucleus n in au. Calculated hyperfine parameters of the nuclei along with experimental values or values obtained from the literature for similar complexes are reported in Table V.

Table V. Hyperfine Coupling Constants, A_n, and Isotropic NMR Shifts, δ, for *trans*-$[Cr(ox)_2(py)_2]^-$

	calcd			exptl	
nucleus	$s_n(0)$,[a] au	10^4A_n, cm^{-1}	δ	10^4A_n, cm^{-1}	δ[b]
^{53}Cr	-3.80×10^{-1}	16.0		16.2–17.0[35]	
^{14}N	-8.98×10^{-2}	−3.01		0.03[37]	
$^1H_1$	-3.58×10^{-4}	−0.178	70		70
$^1H_2$	-8.53×10^{-4}	−0.424	170		−3
$^1H_3$	2.65×10^{-3}	1.32	−520		29
$^{17}O_1$	1.41×10^{-2}	−0.954			
$^{17}O_2$	6.18×10^{-3}	−0.425			
^{13}C	1.42×10^{-3}	0.0887			
$^{13}C_1$	4.34×10^{-4}	0.0271			
$^{13}C_2$	-4.04×10^{-3}	−0.252			
$^{13}C_3$	-5.05×10^{-3}	−0.316			

[a] Spin density at the nucleus. [b] Taken from deuteron NMR data.[3] Note that the isotropic NMR shifts are obtained by subtracting the chemical shift given in Table I from 7 ppm (the approximate chemical shift of the free pyridine ligand). This is opposite to the sign convention used in Table I.

The computed ^{53}Cr hyperfine coupling constant, 16.0×10^{-4} cm^{-1}, is typical of experimental values found in a wide variety of Cr(III) complexes and may be within a few percent of the true value.[29,35] The value reported here compares well with the value of 16.2×10^{-4} cm^{-1} reported for Cr(III) doped into $Co(en)_3Cl_3 \cdot NaCl \cdot 6H_2O$.[35]

There is a diverse set of deuterated pyridine-containing Cr(III) complexes which all have very similar ^2H NMR spectra,[36] as was noted previously. The calculated and experimental values for the protons of *trans*-$[Cr(ox)_2(py)_2]^-$ are reported in Table V. The value calculated for H_1 (2(6)-position) is identical with the experimental value, but the computed shifts at H_2 and H_3 (3(5)- and 4-positions) are as much as 2 orders of magnitude too large and of the wrong sign. The proton NMR shifts of Fe(II) porphine when calculated according to McConnell's relation[28] were found to give reasonable agreement with experiment.[7] For this Cr(III) complex, McConnell's relation $a_H = -Q\rho_\pi$ (with $Q = 21.0 \times 10^{-4}$ cm^{-1} and the ρ_π = carbon spin populations) gives the contact shifts of the hydrogens at the 2(6)-, 3(5)-, and 4-positions to be 3, 19, and 230 ppm, respectively, which is still in poor agreement with experiment.

The computed ^{14}N hyperfine coupling constant is 2 orders of magnitude larger and is of opposite sign from the value reported by McGarvey and Pearlman for $[Cr(py)_2(H_2O)_4]^{3+}$.[37]

We believe that the poor results are a consequence of mixing of the formally unoccupied Cr $3d_{z^2}$ orbital (σ bonding with respect to pyridine) with the singly occupied Cr $3d_{x^2-y^2}$ orbital, which leads to a large error in the spin polarization within the a_g symmetry block. For an octahedral Cr(III) ion, it is expected that spin should enter the pyridine through the interaction of the pyridine π orbitals with the Cr $3d_{yz}$ orbital (π bonding with respect to pyridine). Two factors determine whether the spin density will be anomalous. First, the symmetry of the complex determines whether the singly occupied and unoccupied metal d orbitals are allowed to mix. Second, since the energies of the metal d orbitals are depressed into the range of the ligand MOs which would otherwise be mismatched in energy, mixing of the Cr $3d_{z^2}$ orbital into the wave function is particularly favorable. The $13a_g$ MO, which is delocalized over the entire pyridine ligand and has 16% of the charge

(33) Kurland, R. J.; McGarvey, B. R. *J. Magn. Reson.* **1970** *2*, 286.
(34) Jesson, J. P. In "NMR of Paramagnetic Molecules"; Lamar, G. N., Horrocks, W. D., Jr., Holm, R. H., Eds.; Academic Press: New York, 1973; Chapter 1.
(35) McGarvey, B. R. *J. Chem. Phys.* **1964**, *41*, 3743.
(36) Note that Fermi contact shifts are independent of the magnetic moment of the nucleus and both ^2H and ^1H NMR spectra are quite similar.
(37) McGarvey, B. R.; Pearlman, J. *J. Magn. Reson.* **1969**, *1*, 178.

on the Cr ion, lies about 2 eV below the singly occupied Cr 3d orbitals and may be responsible for the poor results.

Quantitative errors in spin densities at the nuclei do occur in systems such as the M(II) porphines, but these errors are apparently small compared to what happens in *trans*-$[Cr(ox)_2(py)_2]^-$. Mechanisms that disperse spin into the ligand by a qualitatively incorrect mechanism are forbidden in Cu(II) and Ag(II) porphines because of the orbital occupations and in Fe(II) porphine by symmetry. This conjecture is further supported by a calculation in which the d_{z^2} partial wave on the Cr atom was removed from the wave function. This calculation could only be converged to 10^{-3} in the potential, but the spin populations of the hydrogen atoms show the same trend in chemical shifts as is observed experimentally. Since 93–95% of the total spin populations on the hydrogen atoms is contributed by the σ orbitals, it is believed that the low metal d-orbital energies are the principal cause of the problem.

Calculations using larger empirical metal sphere radii tend to have metal d-orbital energies about 1 eV higher than in calculations using Norman radii.[6] How this affects magnetic properties, however, has not been described. It would be interesting to compare our results by the Norman procedure with new calculations using the empirical radii. This choice of radii will undoubtedly raise the Cr(III) d-orbital energies, but it may not be sufficient to improve the magnetic properties to an extent that is useful for chemical applications to low-symmetry Cr(III) complexes.

Conclusions

The Xα–SW method is a valuable tool for describing the electronic and magnetic properties of Cr(III) compounds. However, serious errors should be expected when ligand to metal (and metal to ligand) charge-transfer transitions are described, as is the case with other first-row transition metals. The anomalously low energies of the metal d orbitals tend to match the formally unoccupied metal d orbitals with ligand MOs. In transition-metal complexes of low symmetry where singly occupied and empty metal d orbitals belong to the same irreducible representation, large errors can be expected for hyperfine interactions. The mixing of singly occupied and empty metal orbitals along with the energy match of the ligand MOs with the metal d orbitals allows spin into the ligand through channels that would normally not be available.

Acknowledgment. We gratefully acknowledge Dr. D. A. Case for helpful discussions, Dr. J. G. Norman for instruction on using the Xα programs, J. I. Legg (thesis advisor to W.D.W.), and both the National Institutes of Health (Contract No. GM23081-06) and the U.S. Department of Agriculture (Contract No. 82-CRCR-1-1005) for partial support of this work.

Registry No. *trans*-$[Cr(ox)_2(py)_2]^-$, 36444-16-3; ^{53}Cr, 13981-78-7.

Contribution from the Institute of Inorganic Chemistry, University of Cologne, D-5000 Köln 41, West Germany

Joint Bond Breaking in the Photolysis of the Tris(1,3-diaminopropane)chromium(III) Ion

E. GOWIN and F. WASGESTIAN*

Received May 30, 1984

The photoaquation of $[Cr(tn)_3]^{3+}$ (tn = 1,3-diaminopropane) was studied in acid and alkaline solution by means of absorption spectroscopy, ion-exchange chromatography, pH measurements, acid–base titrations, phosphorescence intensity studies, and determination of free tn. The data indicate two parallel photochemical reaction paths leading to $[Cr(tn)_2(H_2O)(tnH)]^{4+}$ and $[Cr(tn)_2(H_2O)_2]^{3+}$ with quantum yields of 0.14 and 0.04, respectively.

Introduction

To substitute a bidentate ligand, two coordination sites have to be replaced. For many compounds the final detachment of the ligand is much faster than the breaking of the first bond. Therefore, one-ended species often escape detection. As far as the thermal aquation of chromium(III) diamine complexes is concerned, several studies[1-5] succeeded in identifying one-ended species. Especially in the well-studied $[Cr(en)_3]^{3+}$ system (en = 1,2-diaminoethane) the $[Cr(en)_2(enH)(H_2O)]^{4+}$ ion had been found to be the thermal[2] as well as the photochemical[5] reaction product.

Complexes with 1,3-diaminopropane (tn) are kinetically more stable than en complexes.[6-8] This property contradicts expectations, which considered five-membered chelate rings to be more stable than six-membered ones.[9]

The importance of the ring size in photochemical reactions of chromium(III) chelate complexes has not been given much thought, yet.[10] $[Cr(tn)_3]^{3+}$ provides an appropriate object for the purpose of studying the influence of ring size, because the spectral characteristics of $[Cr(tn)_3]^{3+}$ are very similar to those of $[Cr(en)_3]^{3+}$ and other CrN_6 systems. Hence, in solution any difference in photochemical reactivity have to be attributed to steric effects.

In his thesis Cimolino[6] reported some experiments on the thermal and photochemical reactivity of $[Cr(tn)_3]^{3+}$ as a supplement to his study of the stereophotochemistry of $[Cr(en)_3]^{3+}$. Our study gives further information about the $[Cr(tn)_3]^{3+}$ system concerning the mechanism of the detachment of a bidentate ligand.

Experimental Section

$[Cr(tn)_3]Cl_3$ was prepared according to Pedersen.[11] It was transformed to the perchlorate salt by repeated precipitation (three times) from aqueous solution. *cis*-$[Cr(tn)_2(H_2O)_2](NO_3)_3 \cdot H_2O$ was obtained by the method of Nakano and Kawaguchi.[12] Purity was checked by visible spectra, IR spectra, and elemental analysis (C, H, N, Cr).

All visible spectra were recorded with a Cary Model 14 instrument. Additional spectroscopic measurements were accomplished on a Zeiss PMQ II. Absorbed quanta were recorded by a thermostated bolometer apparatus described elsewhere.[13] pH changes were determined with a

(1) Childers, R. F.; Vander Zyl, K. G.; House, D. A.; Hughes, R. G.; Garner, C. S. *Inorg. Chem.* **1968**, *7*, 749.
(2) Mønsted, L.; Mønsted, O. *Acta Chem. Scand., Ser. A* **1975**, *A29*, 29.
(3) Mønsted, L. *Acta Chem. Scand., Ser. A* **1976**, *A30*, 599.
(4) Fukuda, R.; Walters, R. T.; Mäcke, H.; Adamson, A. W. *J. Phys. Chem.* **1979**, *83*, 2097.
(5) Cimolino, M. C.; Linck, R. G. *Inorg. Chem.* **1981**, *20*, 3499.
(6) Cimolino, M. C. Thesis, University of California at San Diego, 1982.
(7) DeJovine, J. D.; Mason, W. R.; Vaughn, J. W. *Inorg. Chem.* **1974**, *13*, 66.
(8) Couldwell, M. C.; House, D. A. *Inorg. Chem.* **1972**, *11*, 2024.
(9) Basolo, F.; Pearson, R. G. "Mechanismen in der anorganischen Chemie"; Georg Thieme Verlag: Stuttgart, West Germany 1973; p 186.
(10) Zinato, E. "Concepts of Inorganic Photochemistry"; Adamson, A. W., Fleischauer, P. D., Eds.; Wiley: New York, 1975.
(11) Pedersen, E. *Acta Chem. Scand.* **1970**, *24*, 3362.
(12) Nakano, M.; Kawaguchi, S. *Bull. Chem. Soc. Jpn.* **1979**, *52*, 3563.

0020-1669/85/1324-3106$01.50/0